Novel computational method for accurate determination of the effective conductivity and the local field of multicomponent 3D composites

2004 J. Phys. A: Math. Gen. 37 5679

(http://iopscience.iop.org/0305-4470/37/21/013)

INSTITUTE OF PHYSICS PUBLISHING JOURNAL OF PHYSICS A: MATHEMATICAL AND GENERAL

J. Phys. A: Math. Gen. **37** (2004) 5679–5687 PII: S0305-4470(04)65117-1

Novel computational method for accurate determination of the effective conductivity and the local field of multicomponent 3D composites

Lotfi Zekri[1], **Nouredine Zekri**[1] **and Jean Pierre Clerc**[2]

[1] USTO, Département de Physique, LEPM, BP 1505 El M'Naouar, Oran, Algeria
[2] EPUM, Technopôle Château Gombert, 5, Rue Enrico Fermi 13453 Marseille, France

E-mail: nzekri@yahoo.com

Received 21 June 2003, in final form 1 March 2004
Published 12 May 2004
Online at stacks.iop.org/JPhysA/37/5679
DOI: 10.1088/0305-4470/37/21/013

Abstract

We present a new numerical method solving exactly Kirchhoff laws to determine the effective ac and dc conductivity and the local field for large scale 3D composites with any number of components. This method is an extension of a previous one restricted to 2D and two-component composites. It is much slower than the Frank and Lobb method for conductivity but calculates in addition exactly the local field for 3D systems with large sizes (which was not done by any previous method). The local field enhancement obtained by this method is in good agreement with recent experimental results and is two orders of magnitude lower than the values obtained by a widely used real space renormalization group method. We further discuss some 3D example calculations of impedance spectra and Cole and Cole diagrams for a three-component sample as well as the local field at the surface plasmon resonance.

PACS numbers: 02.70.−c, 84.37.+q, 51.70.+f, 83.80.Ab, 78.20.−e

1. Introduction

Recently, there has been increasing interest in nonlinear optical properties of composite materials due to field enhancement [1]. In addition, effective ac conductivity [2] and impedance spectra have wide applications in various fields of science and technology [3] where materials and composites can be modelled by RLC networks to characterize their dielectric and magnetic properties. The use of Kirchhoff laws is the direct way to compute both impedance and local field in such networks. However, this corresponds for large systems to matrices of sizes as large as the square of the system size, rapidly exceeding computer capacity. Therefore, all previous methods avoided directly solving Kirchhoff equations, using either approximations or recursive methods but at the cost of losing information on the local field in each node

(or equivalently the current in the branches). One of the rare methods yielding the local field is the real space renormalization group (RSRG) technique, initially introduced by Bernasconi [4], presenting the 2D network as a network of Wheatstone bridges which is reduced in each step to a smaller network, up to obtaining only one branch with the effective impedance. The inverse transformations yield the local field. This transformation changes each mesh of four branches to a bridge of five branches, introducing twice an extra branch, which sensitively affects the results. This method is very fast and useful for effective conductivity (or impedance) calculations. However, although the local-field calculations were never checked, this method was extensively used for the computation of local-field distribution, which was found very large with significant consequences for Raman scattering and nonlinear optics [5]. Recent experimental results on near-field investigations showed that local-field fluctuations are much lower [6].

In a previous paper [7], we proposed a new numerical method for exactly solving Kirchhoff laws for large 2D systems and yielding both impedance (or conductance) and the local field. Although slower, this method provides exactly the same results as the Franck and Lobb method [8] (which is a transformation from stars to triangles or vice versa in a network) for conductance calculations as well as the critical exponents at the percolation threshold. We found the maximum local-field enhancement two orders of magnitude smaller than the results obtained by the RSRG method but in agreement with the recent near-field measurements. However, most real materials are mainly three-dimensional and have more than two components, so that all previous numerical interpretations of experimental results remain approximations. It is then important to study such effects by investigating 3D networks numerically.

To this end, we expand in this paper our previous algorithm to three dimensional systems with more than two components. The next section will be devoted to the description of the method, while in section 3, we present some example calculations on both impedance spectra and local-field distribution near the resonance frequency where this field is expected to be larger.

2. Description of the method

Let us first recall the calculation method for 2D systems, and then expand it to three dimensions. We consider a general RLC network where two different kinds of bounds (for instance LR and C) are randomly placed in a 2D square lattice of size $N \times N$ with a concentration p of one kind (e.g., the inductive one) which is at the bond percolation threshold (0.5), i.e. the minimum concentration of metallic components leading to the appearance of a path connecting the two ends of the sample [9]. We apply a voltage V (e.g., unity) between the ends of the system (see figures 1). In general two shapes of the lattice are used in this problem: one, shown in figure 1(a), in which the ends are parallel [8], and the other one, shown in figure 1(b), in which the two ends are perpendicular [4, 5]. The second kind of lattice has only two branches connecting the edges independently of the size of the system. Therefore, the percolation threshold will be much smaller in this case. We limit ourselves, then, to the first kind of lattice (figure 1(a)). A 2D lattice of size N has $N^2 + (N-1)^2$ bonds and $N(N-1)$ nodes.

The aim of this method is to determine the effective conductance σ_{eff} (which is the current incident to the lattice if the conductances are normalized to an applied voltage 1 V) or equivalently the impedance, and the local field in each node. We use to this end the Kirchhoff

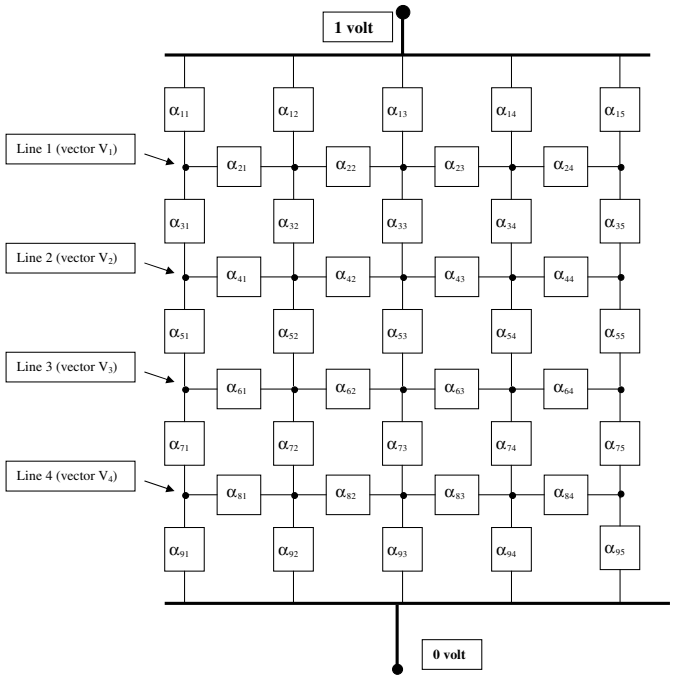

(*a*)

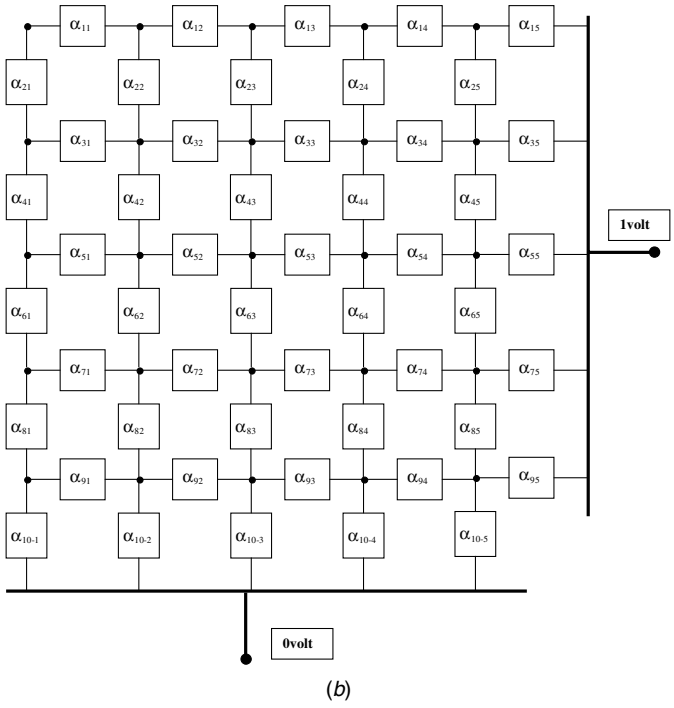

(*b*)

Figure 1. Sample of a 2D lattice of size 5. The voltage is put on (*a*) parallel sides and (*b*) perpendicular sides.

equations at each node i, j (the conservation law of the currents entering the node (i, j)):

$$\sum_{k,l}(V_{k,l} - V_{i,j})\sigma_{k,l}^{i,j} = 0 \tag{1}$$

where the sum is over the nodes of coordinates (k, l), nearest neighbours of nodes of coordinates (i, j) having conductivities $\sigma_{k,l}^{i,j}$. For the nodes connected to the edges of the lattice we replace the node potential $V_{k,l}$ with the corresponding voltage (1 or 0). We have then M equations ($M = N(N-1)$) of M unknown potentials. We can rewrite equation (1) in the following matricial form:

$$\widetilde{\Gamma}\vec{V} = \begin{pmatrix} P_{11} & P_{12} & 0 & \ldots & 0 \\ P_{21} & P_{22} & P_{23} & \ldots & 0 \\ \ldots & \ldots & \ldots & \ldots & \ldots \\ \ldots & \ldots & P_{N-1,N-2} & P_{N-1,N-1} & P_{N-1,N} \\ \ldots & \ldots & 0 & P_{N,N-1} & P_{N,N} \end{pmatrix} \begin{pmatrix} V_1 \\ V_2 \\ \ldots \\ V_{N-1} \\ V_N \end{pmatrix} = \begin{pmatrix} S_1 \\ S_2 \\ \ldots \\ S_{N-1} \\ S_N \end{pmatrix}. \tag{2}$$

In this matrix equation, the matrix $\widetilde{\Gamma}$ is tri-diagonal symmetrical with $(N-1) \times (N-1)$ elements $P_{i,j}$ themselves matrices of dimension $N \times N$ consisting of combinations of the branch conductivities corresponding to currents either in the line i (diagonal elements) or coming to line i from the neighbouring lines ($i \pm 1$) from equation (1). Therefore, only at most three of the matrix elements $P_{i,j}$ do not vanish in each line i. In equation (2) there are $N-1$ elements V_i which are vectors of size N. These elements are the potentials of the nodes of the line i. The elements S_i are vectors of the same size as V_i and vanish except for S_1, which corresponds to the edge at 1 V. The matrices P in equation (2) appearing in the diagonal region of the mother matrix have also a tri-diagonal symmetric form while those outside the diagonal region are diagonal. Indeed, from equation (1), the diagonal elements of $P_{i,i}$ correspond to the sum (with a minus sign) of the conductivities connecting each site of the line i to its neighbours, while the off-diagonal elements are the conductivities of these neighbours.

To solve this matrix equation, it is impossible for large systems to handle directly the mother matrix involved in equation (2) since it means for example for a lattice size 250×250 the use of a memory of about 125 Gigabytes for double precision complex variables. We then partially re-linearize this equation so that we get a set of $N(N-1)$ matrix equations using the matrices P and the vectors V and S described above:

$$\sum_j P_{i,j}V_j = S_i. \tag{3}$$

We solve this set of equations by the substitution method where, starting from the line $i = N$, we obtain in each step the vector V_i related to V_{i-1} up to the equation for $i = 1$ where V_1 is determined. We then use the inverse procedure to determine the other V vectors (and then the local field). The effective conductivity is the sum of the elements of V_N (see figure 1(a)). This inverse procedure needs the storage of all the combinations of matrices involved during the substitution steps. We store less than $3N$ matrices of size $N \times N$ to solve this set of equations. Although the quantity to be stored is very large for large systems, it is N times smaller than that stored by the use of the complete mother matrix. We still need a very high memory for this storage. We store these matrices on a hard disk and the P matrices in RAM memory. For example, for a sample size 250×250 we use a RAM memory of about 12 Megabytes and a computation time for one sample of about 18 min with a Pentium IV 2 GHz. Therefore, it is possible with this method to reach sizes as large as 250×250 on a single PC computer with a reasonable computing time which was not possible with the usual exact methods (except for the Frank and Lobb method which is restricted to the conductivity).

In order to check our results we calculate systematically the incident and the outgoing currents which are always identical up to the last decimal. This is not the case for other approximative methods such as the RSRG method which do not show current conservation.

Let us now extend this method to three dimensions. The system is then composed of N faces (planes) of size $N \times N$. In this case, the network remains as in figure 1(a) for each plane but with nodes connecting between planes. Therefore, if we use equation (1), the sum of the currents entering a node is that of its neighbours in the same plane to be added to its neighbours from the previous and the next plane. This means that Kirchhoff equations remain the same as for 2D lattices, but we add for each node two links to its neighbouring planes. In this case the matrix $\widetilde{\Gamma}$ in equation (2) becomes P_{ii} in the new mother matrix and represents the neighbours in the plane (instead of the line) and remains in the diagonal region ($N(N-1)$ elements), while we add diagonal matrices at the two sides of the diagonal region (P_{ii}) representing the connections to the neighbouring planes (as for the lines in the 2D case). Therefore, equation (2) applies in 3D systems but the mother matrix in the 2D case becomes a block matrix in the diagonal region of the new mother matrix. In other words the new block matrices in the new mother matrix are now tri-diagonal matrices in the diagonal region and diagonal ones immediately at the two sides of the diagonal region. The same procedure stays as it is for solving the new system of equations involving such new block matrices. We store in this case less than $3N$ such new matrices in RAM memory while the intermediate matrices are stored on the hard disk as for 2D matrices. The three-dimensional system can then be mapped into 2D faces connected to one another by their nodes.

With this method, a calculation with a sample size $45 \times 45 \times 45$ takes 5 h and uses 250 MB RAM memory on a Pentium IV 2 GHz (in fact the computational time remains unchanged with a weaker computer since the major time is used for storing large matrices in the hard disk whose time access is of the order of the running time). Note that this time is proportional to $N^2(N-1)$ since the substitution process is used for the whole nodes. Therefore, if we double the size, the computation time will be multiplied by 8.

The number of kinds of components to be used in the sample does not affect the organization of the above described computation. For two components, we should generate through the sample two kinds of elementary ac conductivities with probabilities p and $1-p$ respectively for each one. For three components, we generate three different conductivities with probabilities p, q and $1-p-q$, and so on. The remaining calculations do not change. We can then generate samples with any number of components.

Finally, it should be noted that this model is limited to frequencies where the electric field wavelength is much larger than the size of the components. In the case of systems of around centimetre size, one should be careful when using frequencies of the order of a GHz. Indeed, in this case, the electric field should be viewed as a wave with transmission and refection probabilities, and Maxwell's equations are needed.

3. Results and comparisons

In the previous paper, we have extensively discussed the comparison of our method for ac and dc conductivity in 2D systems with the Franck and Lobb (FL) method [8], and found exactly the same results as well as the critical exponents. We have also compared the results on the local field distribution with those of the RSRG method for 2D systems. Since the literature provides numerical and theoretical data on 2D systems, we compare in this section the frequency-dependent impedance and local field for 2D and 3D systems in order to explain the experimental results.

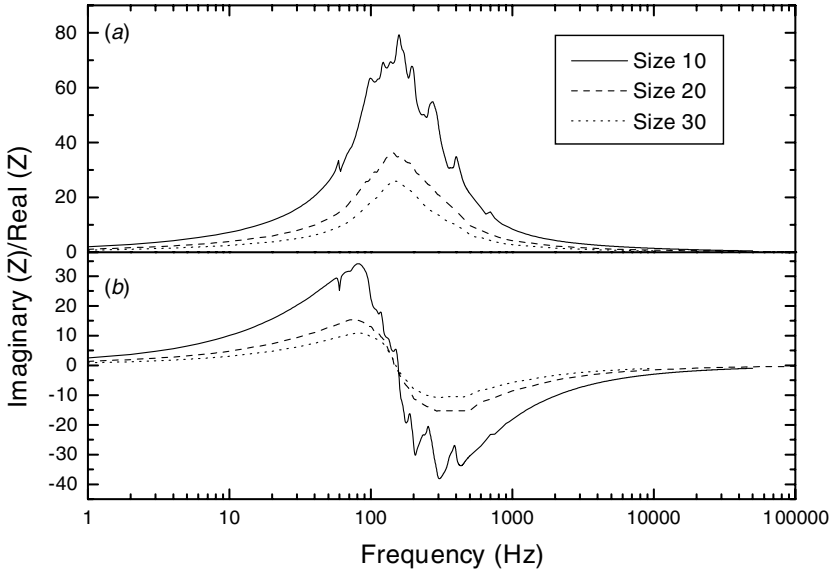

Figure 2. Frequency dependence of the real part (*a*) and imaginary part (*b*) of the impedance versus frequency for a 3D system of three components $R = 30\,\Omega$, $L = 400\,\mathrm{mH}$ and $C = 1\,\mu\mathrm{F}$, with the same proportion $(1/3)$. Three different sizes are used: 10, 20 and 30.

3.1. Impedance spectra calculations

Let us examine now as an example the impedance spectra, for three-component networks where we have in each branch, with the same probability $1/3$, either an R component of value $30\,\Omega$, a purely inductive component L of $400\,\mathrm{mH}$ or a purely capacitive component of $1\,\mu\mathrm{F}$. Such a proportion $(1/3)$ is near the percolation threshold for three-dimensional dc currents and is chosen because of the possibility of having an infinite cluster for each component. The presence of a resistance and capacitance yields a relaxation frequency while additional inductive components will introduce another characteristic frequency (the resonance frequency).

In figure 2, we show for 3D systems the frequency dependence of the effective complex impedance (its real and imaginary parts) for different system sizes and for a sufficiently large frequency band where both characteristic frequencies are shown. The resonance frequency ω_{res} corresponds to the maximum of the real part of the impedance (or equivalently when the imaginary part vanishes). The relaxation frequency ω_{rel} corresponds to the minimum imaginary part of the impedance in its capacitive region (where the imaginary part is negative). In these figures, some resonance peaks appear for small sizes both in the real and imaginary parts of the effective impedance. They correspond to local resonance and relaxation frequencies due to the random organization of the components in each cell of the system. Indeed, in small systems the components are inhomogeneously distributed in the sample so that the spectrum is constituted of a set of resonances obtained from local configurations which influence sensitively the spectra if their quality factor $\left(Q = \frac{1}{R}\sqrt{\frac{L}{C}}\right)$ is large. When the size increases, the impedances decrease and the curves become smoother and the local resonances disappear while only one characteristic frequency remains for each kind (ω_{res} and ω_{rel}) which seems not to depend on the size (as shown in figures 2 for sizes 20 and 30).

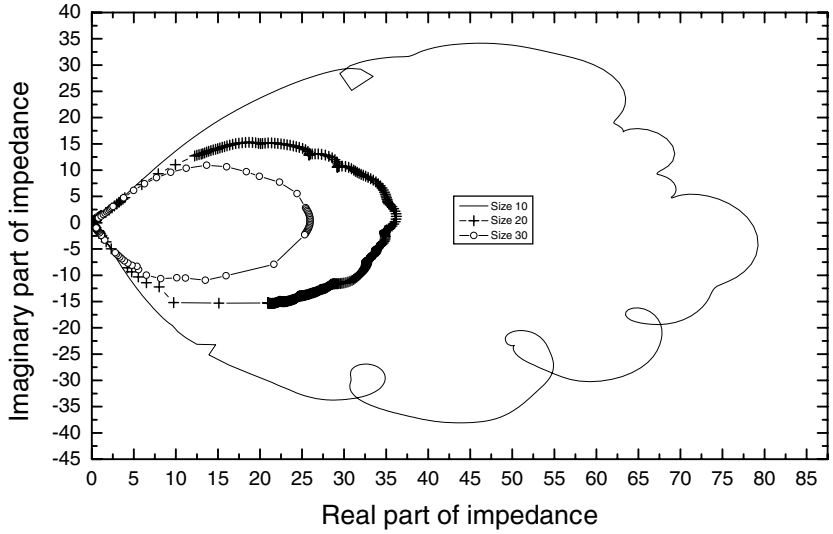

Figure 3. Cole and Cole diagram for the same parameters as in figure 2.

This smoothness for larger sizes is observed in the Cole and Cole diagram for this system (see figure 3), where the loops corresponding to the local resonances shown for the size 10 disappear for larger sizes. It is important to note in this figure that the impedance seems not to be affected by the size for very large or very small frequencies, while the dependence on size is very significant for intermediate ones. The curve will saturate for very large sizes, where effective medium theory predicts its behaviour. Note here that in 3D systems, we seem to reach the effective medium behaviour more rapidly than for 2D systems (not shown here), where some local resonances still appear in the spectrum even for sizes as large as 200×200.

The resonance frequency here is around 150 Hz for all the simulated 3D cases, while that predicted by the effective medium theory for 2D systems is 251 Hz. We explain this difference by the effective local topology of the 3D network, where the unit cell contains more R, L and C components than in 2D systems. This local topology seems to allow the resonance frequency to be about $\sqrt{3}$ lower than in 2D systems.

3.2. Local field

In this section, we show the local field distribution for 3D systems and compare it with the results in 2D systems. In the previous paper [7], we have found that the local field is two orders of magnitudes lower than the RSRG calculations predict. As discussed above, the recent experimental results are in agreement with our results. It should be noted that the experimental measurements are not on exactly two-dimensional systems, but the thickness can sensitively affect the results. Therefore, it is interesting to examine the behaviour of the local field for three-dimensional systems.

In figure 4, we compare the probability distribution of the local field for 2D (200×200) and 3D ($30 \times 30 \times 30$) systems at the resonance frequency (corresponding to the vanishing imaginary part of the effective impedance). For both systems, we use three components R, L and C with the same proportion $(1/3)$. The resonance frequency for the corresponding 2D system is 245 Hz, while for a 3D system this frequency is 149 Hz. We see from this figure that the most probable local field for 3D is one order of magnitude larger than in 2D. The

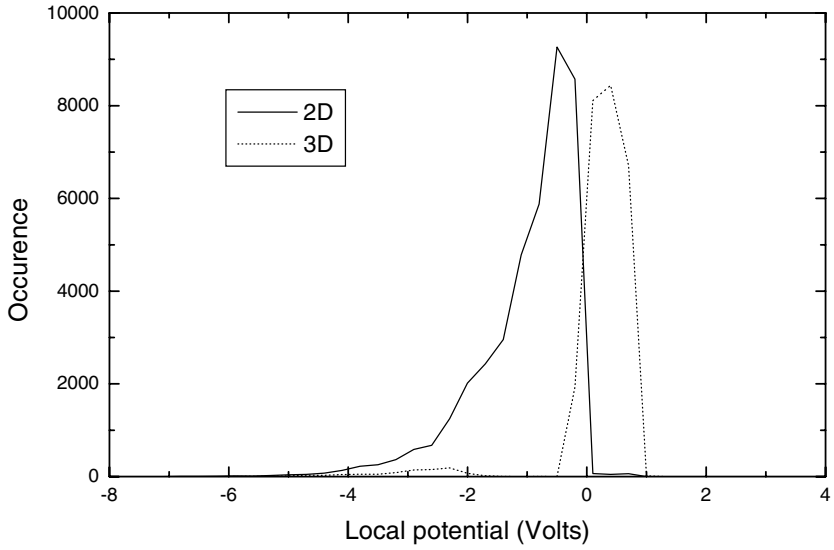

Figure 4. The probability distribution of the local field for the same parameters as in figure 2 at the resonance frequency for 2D systems (of size 200) and 3D systems (of size 30).

maximum value of the field seems to be slightly larger in 3D systems. This increase is due to the existence of a larger resonating cell in 3D, where above a critical thickness it enhances the field. Therefore, the field may be slightly enhanced in the previous near-field measurements [6] if the films used are thicker, but the 'hot' regions remain still of the same magnitude as our previous calculations. We note here that such 'hot' regions can be enhanced if we significantly decrease the dissipation R.

4. Conclusion

We have presented (in the frequency range where Kirchhoff laws are applicable) exact calculations of the complex impedance and local field for multicomponent three-dimensional systems. This method allows the investigation of the behaviour of such quantities (particularly the local field) for finite systems, while the existing models provided only the asymptotic behaviour of the ac conductivity when the size is very large and the system is homogeneous. This method then opens a way for new investigations of size effects as well as the inhomogeneity or asymmetry of the system.

References

[1] Shalaev V 1996 *Phys. Rep.* **272** 61
Sarychev A K and Shalaev V M 2000 *Phys. Rep.* **335** 275
[2] Zeng X C, Hui P M and Stroud D 1989 *Phys. Rev.* B **39** 1063
Zeng X C, Hui P M, Bergman D J and Stroud D 1989 *Phys. Rev.* B **39** 13224
Bergman D J and Stroud D 1992 *Solid State Phys.* **46** 147
[3] Ross Macdonald J 1987 *Impedance Spectroscopy* (New York: Wiley)
Duncan Craig Q M 1995 *Dielectric Analysis of Pharmaceutical Systems* (London: Taylor and Francis)
Clerc J P, Giraud G and Luck J M 1990 *Adv. Phys.* **39** 1063
[4] Sarychev A K 1977 *Zh. Eksp. Teor. Fiz.* **72** 1001
Reynolds P J, Klein W and Stanley H E 1977 *J. Phys. C: Solid State Phys.* **10** 167
Bernasconi J 1978 *Phys. Rev.* B **18** 2185

[5] Sarychev A K, Bergman D J and Yagil Y 1995 *Phys. Rev.* B **51** 5366
Markel V A, Shalaev V M, Stechel E B, Kim W and Armstrong R L 1996 *Phys. Rev.* B **53** 2425
Brouers F, Blacher S, Lagarkov A N, Sarychev A K, Gadenne P and Shalaev V M 1997 *Phys. Rev.* B **55** 13234
Gadenne P, Brouers F, Shalaev V M and Sarychev A K 1998 *J. Opt. Soc. Am.* B **15** 68
Shalaev V M and Sarychev A K 1998 *Phys. Rev.* B **57** 13265
[6] Ducourtieux S *et al* 2001 *Phys. Rev.* B **64** 165403
Gadenne P, Quelin X, Ducourtieux S, Gresillon S, Aigouy L, Rivoal J C, Shalaev V and Sarychev A K 2000 *Physica* B **279** 52
[7] Zekri L, Bouamrane R and Zekri N 2000 *J. Phys. A: Math. Gen.* **33** 649
[8] Frank D J and Lobb C J 1988 *Phys. Rev.* B **37** 302
Lobb C J and Frank D J 1984 *Phys. Rev.* B **30** 4090
[9] Staufer D and Aharony A 1994 *Percolation Theory* 2nd edn (London: Taylor and Francis)